

Modeling Areas Exposed to Radioactive Elements Using Landsat Satellite Images Case Study of Shirkuh Yazd

Mohamad Amin Atapour^{a*}, Seyed Hesamadin Moinzadeh Mirhoseini^b, seyede_Razieh
keshavarz^c

^a Engineering Unit, Kerman Region, National Iranian Oil Refining & Distribution Company, Petroleum Ministry, Kerman, Iran

^b Faculty member of Shahid Bahonar University of Kerman

^c Master of Science in Remote Sensing and GIS

Received 5 February 2019; revised 16 September 2019; accepted 24 September 2019

Abstract

The most important radioactive elements of the crust are uranium and thorium. Different isotopes of these elements become stable elements with long decay chains and the production of other radioactive elements. The Shirkuh granite batholith, with a partial melting origin, extends over a thousand square kilometers, from chronology to early geological formations to the present day. According to the measurement of radionuclides in water, soil and rock, Shirkuh granite has U and Th radioactive elements. Landsat satellite images are used to study the Shirkuh in terms of radioactive elements distribution. Also, 30 kinds with the number of radioactive elements identified by Field Spec were sampled and spectral libraries were designed. In this study, the areas with the highest concentration of radioactive elements were determined using spectral angle mapping and supervised classification. The results show that the highest uranium and thorium specimen are located in three regions: west and south of Manshad and south of Tabriz.

Keywords: Landsat, Shirkuh, Spectroscopy, Radioactive Elements, Uranium and Thorium.

* Corresponding author Tel: +98-9129328324
Email address: maatapour@yahoo.com

1. Introduction

Natural Radionuclides exist in most rocks in lithological formations and units and the most important of these natural radionuclides are ^{238}U , ^{232}Th and ^{40}K (Zia Zarifi et al., 2014). Radiation elements are important from two perspectives. First is their discovery for the use of nuclear power plants and the second is the study of environmental pollution resulting from the excessive standardization of radionuclides in different environments. (Mulloy et al., 2001).

One of the most important effects of the radionuclides radiation is its impact on living tissues, which causes major diseases due to ionizing radiation. The World Health Organization has identified the presence of more than 2 micrograms of uranium per liter of water as potentially hazardous, as the maximum permissible level of uranium in one liter of water is 16 micrograms per liter (Murat and Mojtahedzadeh, 2010).

Some radioactive elements enter the water cycle through various procedures, while uranium and radium are amongst the most pollutants. The amount of uranium in different waters depends on the composition of the rocks, soils, sediments of the path it follows. Accordingly, calculating and quantifying the activity of natural radionuclides in Shirkuh granite rocks is of great importance.

The use of remote sensing technology and the use of satellite data often reduce costs, save time and increase research accuracy (Najafzadeh et al., 2017).

In recent years, remote sensing technology has been able greatly to facilitate such researches by providing digital data from vast areas for automatic and semi-automatic extraction of the properties of phenomena (Chrysafis et al., 2017).

Traditional and typical land and geochemical methods are cumbersome, slow and complex activities that involve a great deal of fieldwork and require sampling, chemical analysis and interpretation. These costs can be reduced by using visible and infrared spectroscopy techniques and integrated with remote sensing data (Atapour et al., 2013).

These techniques and methods are economically viable and cost-effective tools for mapping land resources compared to conventional methods. Therefore, mapping, identifying and preparing various maps are among the applications of remote sensing, especially in situations where the breadth of navigation limits direct study (Salvi et al., 2001).

Accordingly, the reflectance spectroscopy of the various materials eventually leads to the spectral bank preparation. The main purpose of the spectral library is to feed analysis systems and interpret remote sensing data with ground facts. Although many spectral libraries have been published, but since they include in vitro measurements of mineral samples, there are limitations in identifying and separating rocks, especially with low spectral resolution data (Salvi et al., 2001).

Goltapeh et al., in 2018, evaluated OLI data, ALTA reflectance spectroscopy, and the concept of virtual station in mapping soil heavy metal density distribution. The results showed that the distribution map of soil heavy metal density was obtained more accuracy by using the satellite image bands and applying larger coefficient of correlation.

In 2016, in geological studies in the Nigerian Geological Survey Denbu stated the importance of remote sensing. This survey uses Landsat 8 satellite imagery to design geological maps. This study segregates basaltic and rhyolite volcanic rocks using color composite images and band compositions. The results show the high capability of Landsat 8 satellite images in separating rock units and producing geological maps at regional scale. In 2014, Abu al-Khair surveyed uranium minerals in the Egyptian Central Granite Desert using remote sensing and gamma spectrometer data. This study divides Kadabura's young granite into three parts, using false and composite color images and principal component analysis. These three include the southern part where there is uranium depletion, the central part with high uranium and thorium richness, and the northern part with abundant uranium and thorium rich areas. In 2015, Qiu, conducted a modeling of iron concentration and uranium discovery using spectral angle mapping in the Egimicitan region of China. The results of this study demonstrate the value of satellite imagery information for uranium exploration and for detecting changes in iron concentration. Some radioactive elements enter the water cycle through various processes, including uranium and radium. The amount of uranium in different waters depends on the composition of the rocks, soils and sediments that follow. Therefore, calculating and quantifying the activity of natural radionuclides in rocks is very important. Due to subduction and partial melting of continental crust due to the formation of Shirkuh granite in Yazd, conditions exist for non-standard contamination of radioactive elements.

This research is not only important because of using Landsat imagery and the identification of existing areas regarding new radioactive elements, but also scientifically innovative. In this research two kinds of hypotheses are provided as follow, firstly, using Landsat imagery can identify areas with radioactive elements and secondly, the appropriate kind of images suitable to find these elements are Landsat satellite images.

The main purpose of this study is to identify possible areas contaminated by radionuclides of the Shirkuh-Yazd and to identify areas with higher contamination potential emphasizing Laboratory Reflective Spectroscopy and the spectrum analysis of the sample rocks in the region.

2. Materials and Methods

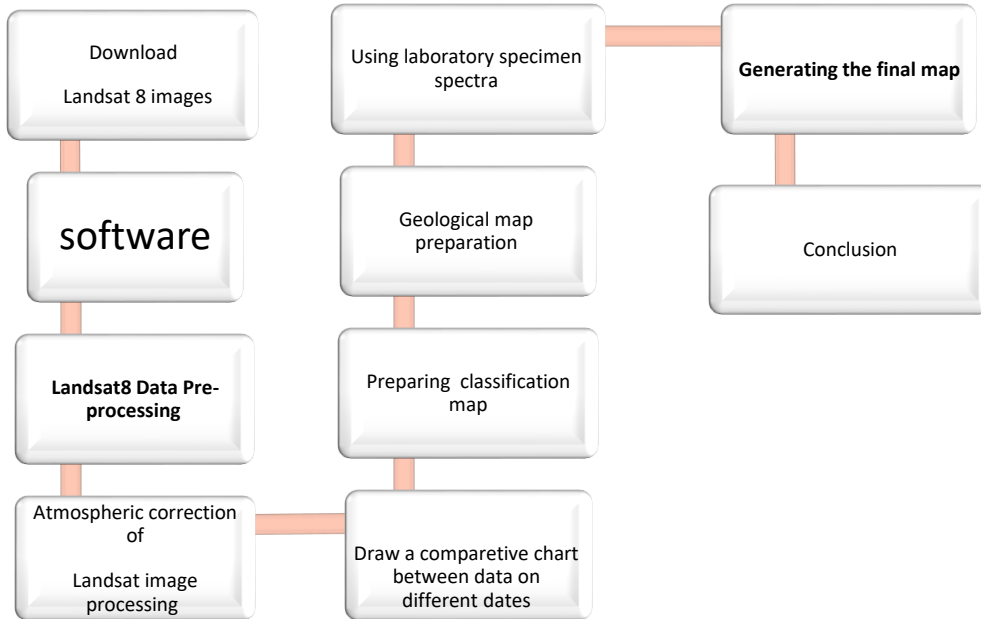


Figure 1. Flowchart

The Shirkuh granite massif area is located 40 km southwest of Yazd and between Taft and Mehriz cities. Geographically, it is located at 246917.35 East and 3493714.54 North and 781799.21 East and 3495962.37 North.

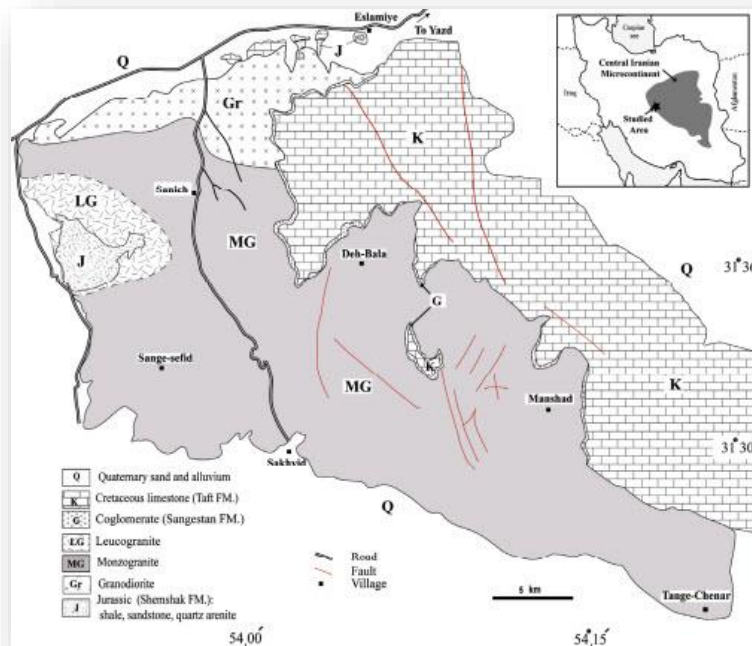


Figure 2. Geological map of different units of Shirkuh rock (Shibi, 2009)

The geology of this area has been associated with the erosion of the Eurasian Plate by the closure of the Paleotectic during the Triassic and the northward movement of central Iran. At the same time with the closure of the Paleotetis in the north, an opening occurred in the Zagros Thrust Zone and a new ocean called the Neotethys. In the Triassic-Jurassic, with the disappearance of Paleotetis in the north, the oceanic crust of the Neotethys began to subduct beneath central Iran (Berberian & king, 1981).

The Paleo-Oceans in Iran, formed after the deluge of the Central Iran-Alborz block from the Arabian Plate in the Late Permian to Early Triassic, transported parts of continents separated from Gondwana to the northern tradition (Guest et al., 2006). Although high-alumina granites originate from partial melting of upper crustal rocks, particularly during continental-continental collision events, in rare cases, they can be produced on the continental active margin by subtracting calc-alkaline series (Villaseca et al., 1998).

Shibi in a study on the petro genesis of Shirkuh peraluminous granitoids more than 200 thin sections of different rock units of the Shirkuh batholith and have been analyzed petrographically. A total of 24 samples from different units were selected for geochemical analysis and elemental analysis was carried out in the Geochemical Laboratory of the Nancy Petrochemical and Geochemistry Research Center of France using the ICP-AES method. The peculiar elements were also analyzed using ICP-MS at the Sabatier Paul University in Toulouse, France. In terms of studying minerals, these rocks have abundant plagioclase (41-35%). Biotite (10 to 15%) is the only mafic mineral in this unit that can be seen in two ways:

1) Sheet and coarse-grained biotites; and 2) fine-grained types surrounded by larger-scale biotites that seem to be fragments of the rosette. Quartz (34 to 37%) was also associated with muscovite and lower amounts of potassium feldspar (12 to 14%) (Shibi, 2009). Compared to other rocks, here, cordierite is associated with a prectytic origin due to the convergence of the chlorite and muscovite assemblage. Zinc, apatite, and monazite are incorporated in biotite only. Ilmenite and small amounts (less than 2%) of tourmaline constitute the sub-minerals of this unit. A thesis on the study of natural radionuclides in Shirkuh granites was sampled from Sazan Abad, Manshad, Banadak Sadat, Tazrjan, Deh-top, Tang Chenar, Zardin, Nair, Sakhvid and Sanich regions and the results were summarized in the table.

Table 1. Special Activity Eq for Granite Samples in Shirkouh Region (Zarei, 2008)

Absorbed Dose Song	Equivalent to radium	Special Activity K40	Special Activity Th232	Special Activity U238 ⁸	sample code
162.5	195.9	844.8	66	36.5	G01
142.5	168.8	802.2	56.1	26.8	G02
148.6	174.9	806.1	59.6	27.6	G03
157.2	203.5	290.6	86.7	57.2	G04
167.8	200.7	919.8	64.8	37.2	G05
139.6	163.1	817.9	53	24.3	G06
138.5	161.2	725	56.7	22.2	G07
159.4	195.1	966	52.8	45.2	G08
157.2	188.7	762.2	66.5	34.9	G09
117.5	135.3	580.1	52.7	15.3	G10
127	158.8	939.7	44.1	23.4	G11
182	211.8	1229.7	59.2	32.5	G12
152.2	176.2	931	56.3	24	G13
168.5	186.7	885.1	61.9	30	G14
162.1	186.9	969.1	61.9	23.8	G15
159.5	185	783.1	71	23.2	G16
161.2	189.5	835	67.4	28.8	G17
159.2	188.7	800.4	67	31.3	G18
145.9	171.5	784.7	59.2	26.4	G19
141.6	168.6	748.9	56.8	27.9	G20
155.4	183.5	698	71.1	28.1	G21
151.9	177.6	857.3	59.7	26.2	G22
132.9	154	880.5	44.9	22	G23
187.6	218.2	931.2	82.5	28.5	G24
166.7	202.4	917.9	62	43.1	G25
164.9	192.4	1001.5	60.6	28.6	G26
143.6	167.8	809.2	56.5	24.7	G27
153.6	178.6	855.1	61.7	24.5	G28
146.6	175.7	797.7	56.6	33.4	G29
156.2	188.4	925.1	54.8	38.8	G30

Thirty existing samples had ²³⁸U specific activity between 15.3 Bq / Kg to 2/57 and the highest specific activity of ²³⁸U was related to G04 code in the western suburbs and the lowest specific activity was ²³⁸U in Shirkuh granite samples related to G10 code in the South of the study area, the east of Tezerjan. Thirty samples had ²³²Th specific activity between 44.1 Bq / Kg to 44/7/86 and the highest specific activity of ²³²Th was related to G04 in the western suburbs and the lowest specific activity was ²³²Th in Shirkuh granite samples related to G11 code in outcrop. The granite is north of Baghi Abad. Thirty existing samples had ⁴⁰K specific activity between 2490 (Bq / Kg) 6/29 to 1229.7 and the highest specificity of ⁴⁰K related to the G12 code in the Upper East 10 granitic outcrop and the lowest ⁴⁰K specific activity in the Shirkuh granite samples. Code G04 is a prominent suburb in the West. Examination of granite samples shows that the absorbed dose values for the samples were between 17.5 (nGy / h) to 187.6 and Most of the absorbed dose in the Sherkuh granite samples is related to the western G24 code and the lowest absorbed dose is related to G10 code southeast of tezerjan.

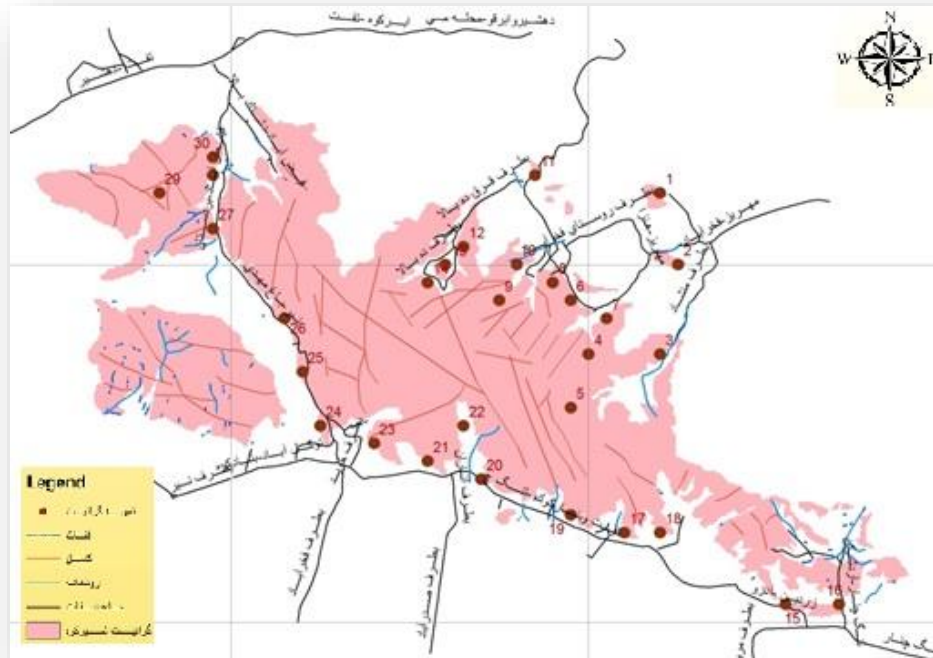


Figure 3. Map of Shirkuh granite massif locations

In this regard, the identification and mapping of rocks from remote sensing data involves a method consisting of various stages of analysis: Image calibration, atmospheric correction, image analysis (statistical or conclusive), Ground approval, verification, fieldwork and final interpretation. Understanding the methods of interfering with electromagnetic radiation with materials and phenomena of the earth will be a complementary tool to these steps and steps. After conducting field studies in the study area and transferring the samples to the lithology and spectroscopy laboratory of Shahid Chamran University of Ahvaz, Reflection of rock samples in the range of visible and short infrared spectra (wavelengths of 350 to 2500 nm and wavelengths of 1 nm in 2151 spectral channels) Measured and recorded using a Field spec 3 ASD¹ spectrometer and RS3 software in the laboratory.

Spectral discontinuities occurred due to the noise from the transition from visible-field detectors to short-IRs 1 and 2 during 1000 and 1800 nm wavelengths that modified by SAMS Software Version 2.3.

(Charts 1 and 2). The Spectral chart recorded by the device (initial chart) containing 2 bounces at 1000 and 1800 nm Chart 1 shows the modified jumping tool in SAMS and the modified graph shown in Chart 2.

¹ - Analytical Spectral Device

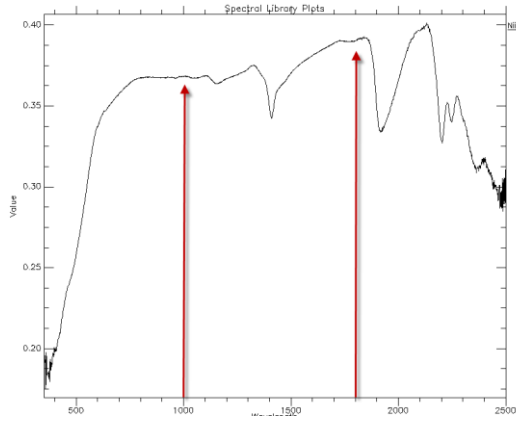


Chart 1. Initial spectral chart

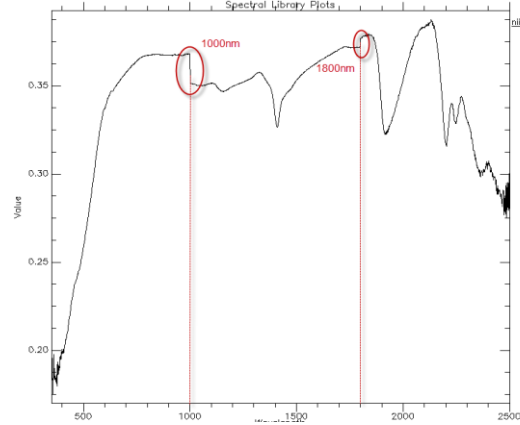


Chart 2. Modified spectral chart

As the Governor's white reference shows almost 98% reflection over all wavelengths (Fields cape Guide 3, 2005; RS3TM Guide, 2005; ASD site). Thus the conversion of the relative reflectance data of the specimens to the absolute reflectance showed very acceptable results that demonstrated the high suitability and capability of the white reference. By converting the relative reflectance of the specimens to absolute reflection in the EXCEL formats available on the ASD site, it was found that the absolute spectrum of the specimens corresponds exactly to the relative spectral graph. Since the standard white reference used reflects nearly 100 percent or one, the two graphs are perfectly consistent. The analysis and characterization of the spectral curves are based on the following parameters that are considered as absorption structures.

1. Wavelength location with the lowest reflectance in absorption bands¹
2. Depth, width, area and asymmetry of bands²
3. Place slope changes and jump points in the curve.³

Adsorption structures in rock samples were analyzed and analyzed by SAMS version 3.2 software and the absorption shapes analysis algorithm, which calculates the absorption rate of each band according to the subsurface area, was applied to the spectra. Diagram 3 shows the spectral difference between the highest and the lowest uranium granite samples. Chart 4 also shows this difference based on the amount of thorium in the sample.

¹- Jump Correction

² - <http://www.asdi.com>

³ -Absorption Feature

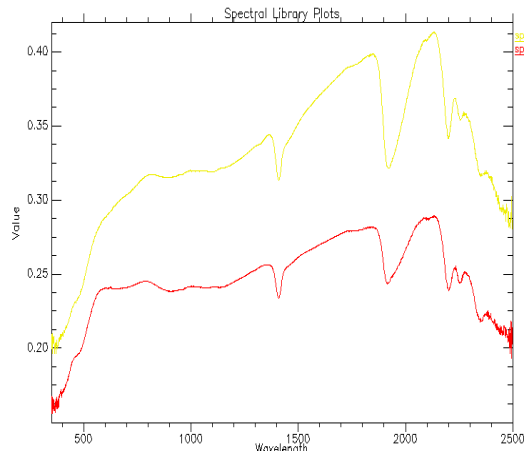


Diagram 4. Comparison between the spectra of the highest and the lowest thorium granites

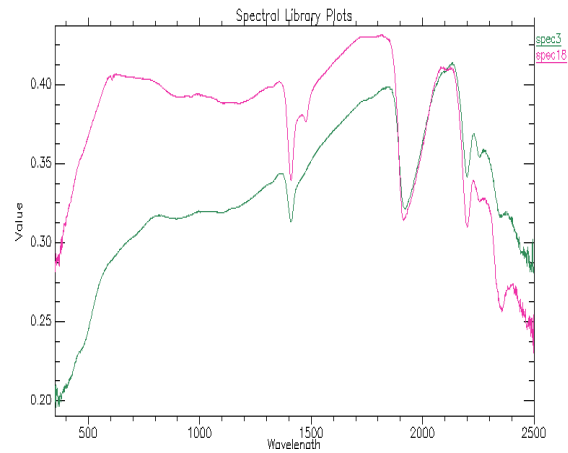


Diagram 3. Comparison between the spectra of the highest and the lowest uranium granites

Classification of rocks by spectral patterns identifies the dominant spectral features of a type of rock or group of rocks. Such spectral segmentation is consistent with the nature of remote sensing sensors and can be the basis for identifying and separating targets in the processing of remote sensing data by predicting the response of spectrometer detectors. This adaptation and simulation can also be performed to investigate the spectral patterns on weathered surfaces in addition to the new surfaces to evaluate the probability and method of identifying and distinguishing this group of rocks in trans-spectral and multi-spectral images. (Longhi et al., 2001).

Absorption feature analysis

The Landslide OLI satellite sensor covers a broad spectral area with 11 bands from the visible to the infrared thermal range with acceptable spatial, spectral and radiometric resolution. Of these 11 bands, 6 bands are within the scope of this study. Its spatial resolution is 30 m in the near-infrared visible range and the short infrared range is separated from the Landscaping Frame Scene (more in Chapter 2), the Shirkuh Granite Range.

Since the purpose of this study was to identify and classify the rocks based on the spectral bank obtained from the recording of spectra in the laboratory, it is necessary to perform the process of converting the digital values recorded by the sensor into radiation and finally reflection.

$$\rho\lambda' = M_{\rho}Q_{cat} + A_{\rho} \tag{1}$$

$\rho\lambda'$ =ToA reflectance, without sun elevation correction

M_{ρ} =Reflectance_MULT_BAND_x, which x is band number

Q_{cat} =Digital Number (DN)

$$\rho\lambda = \frac{\rho\lambda'}{\cos(\theta_{SZ})} = \frac{\rho\lambda'}{\sin(\theta_{SE})} \tag{2}$$

$\rho\lambda$ = ToA reflectance

θ_{SZ} = Sun elevation

θ_{SE} = Angle zenith sun, $\theta_{SZ}=90^{\circ}-\theta_{SE}$

The spectral library was prepared from spectral charts. In this spectral library, each spectrum based on the sampled location has a certain amount of radium from the decay of uranium and thorium. Implementation of the spectral library in the supervised classification will show areas with similar granite composition and radon content. In order to use these spectra in the classification of Shirkuh granites, the spectra need to be modified based on OLI bands. Spectroscopy with Fieldspec3 is very accurate and performs 1 nm in the range of 2500 to 350 nm.

3. Discussion and Results

The use of satellite data considering features like broad and integrated vision, duplicate coverage, the ability to provide timely data and the use of different parts of the electromagnetic spectrum to characterize phenomena has been the subject of great interest by researchers and experts. One of the most important effects of radionuclides radiation is its impact on living tissues, which causes major diseases due to ionizing radiation. Based on the results and comparing this research to the one conducted by Danube in 2016 in Nigeria The importance of remote sensing in geology was highlighted and it was shown that using Landsat imagery could be used for geological mapping and these images, which are used in the present study, have a high ability to detect and distinguish radioactive elements, so using Landsat imagery for similar research can give us plausible results. Using satellite data taking into account properties such as broad and integrated vision, duplicate coverage, the ability to provide timely data and the use of different parts of the electromagnetic spectrum to record the properties of phenomena, It has attracted the attention of many researchers and experts. The most important effects of radioactive materials can be the impact on living tissues, leading to major diseases caused by ionizing radiation. Based on the results obtained and comparing this study with the one conducted by Danube in Nigeria in 2016, the importance of remote sensing in geology was identified and it was shown that Landsat imagery can be used for geological mapping and These images, which have been used in the present study, have a high ability to distinguish and detect radioactive elements. So using Landsat imagery for similar research can give us plausible results.

The spectra obtained from spectroscopy must be converted to L8 image matching spectra. For this purpose, the specimen spectrum was converted to the ASCII file. This file shows the reflection rate at each wavelength. Based on the reflection rate at each wavelength and OLI bands a new ASCII file was created for each granite sample this is illustrated in Figure 5 spectra from spectroscopy and Figure 4 based on OLI bands for Fakhr Abad region.

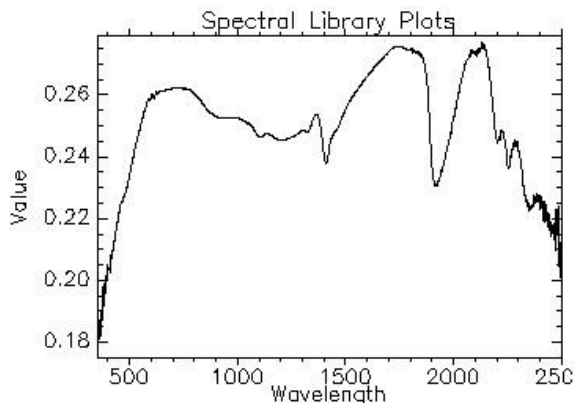


Figure 5. Spectroscopy

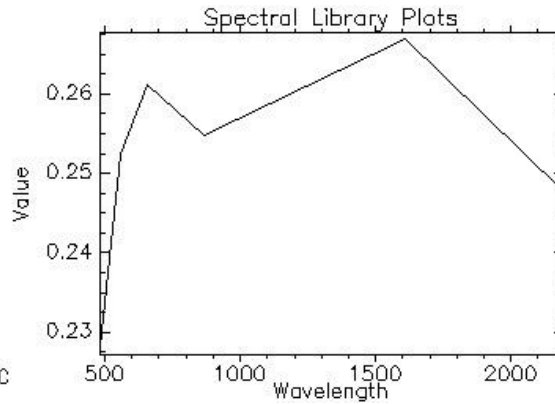


Figure 4. Spectrum based on OLI sensors

After the creation of the new spectral library based on the OLI sensing bands, the supervised classification in ENVI software was performed. Figure 6 is an image from the SAM classification with the spectral library.

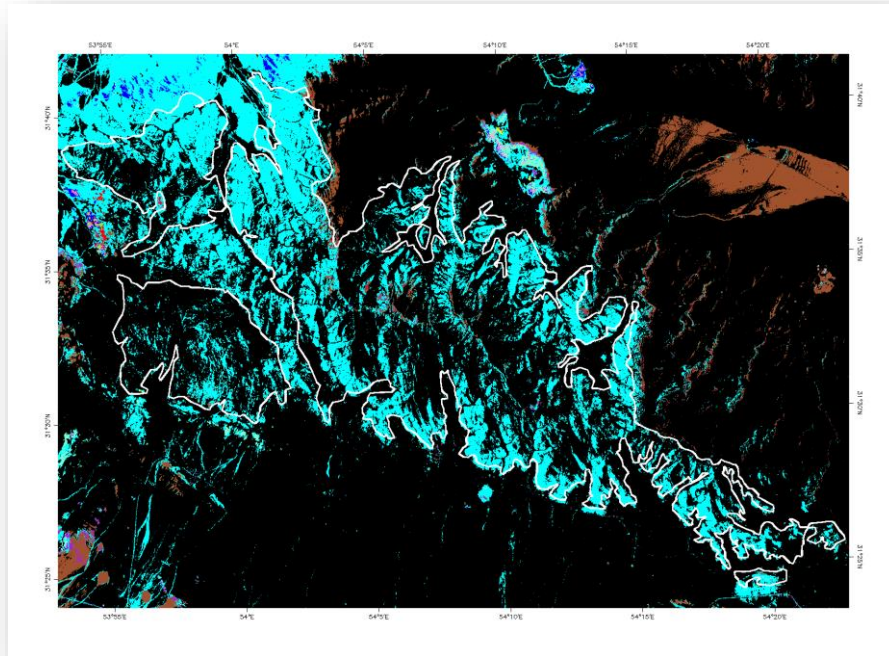


Figure 6. Classification of SAM by spectral library

The spectra obtained from the spectroscopy are very accurate, and the measurements are performed in nm for the full wavelength, but converting them into OLI-compliant bands eliminates much of the spectrum information. The following figures are examples of spectra obtained from spectroscopy and comparison with spectra consistent with OLI sensors. As an example, the spectra of the three areas of Manshad, Fakhri Abad and Chahuk are shown. As is evident in many waves of information, information has been omitted. For example, absorption at the wavelengths 1408 and 1912 as a result of this conversion is completely eliminated and the spectrum is converted to a horizontal line.

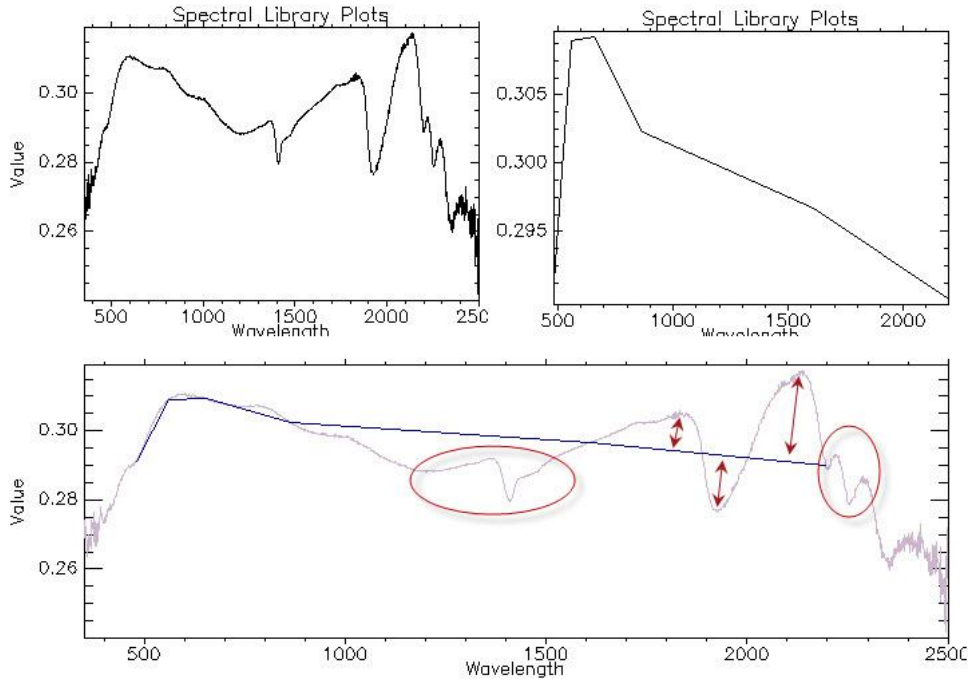


Figure 7. Comparison of the spectra of the Manshad sample

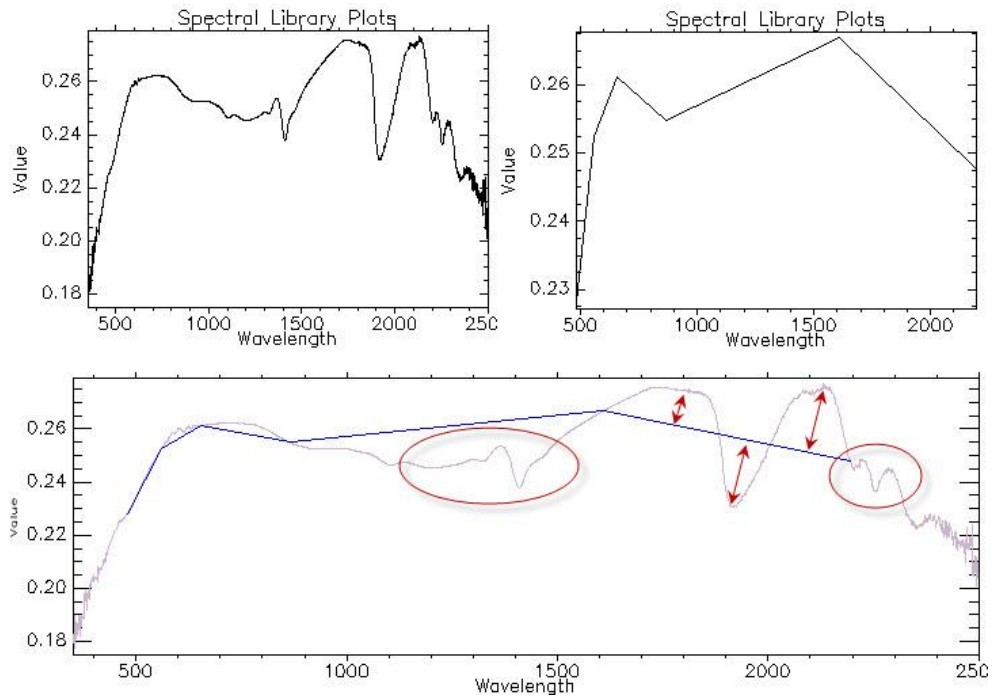


Figure 8. Comparison of Fakhr Abad sample spectra

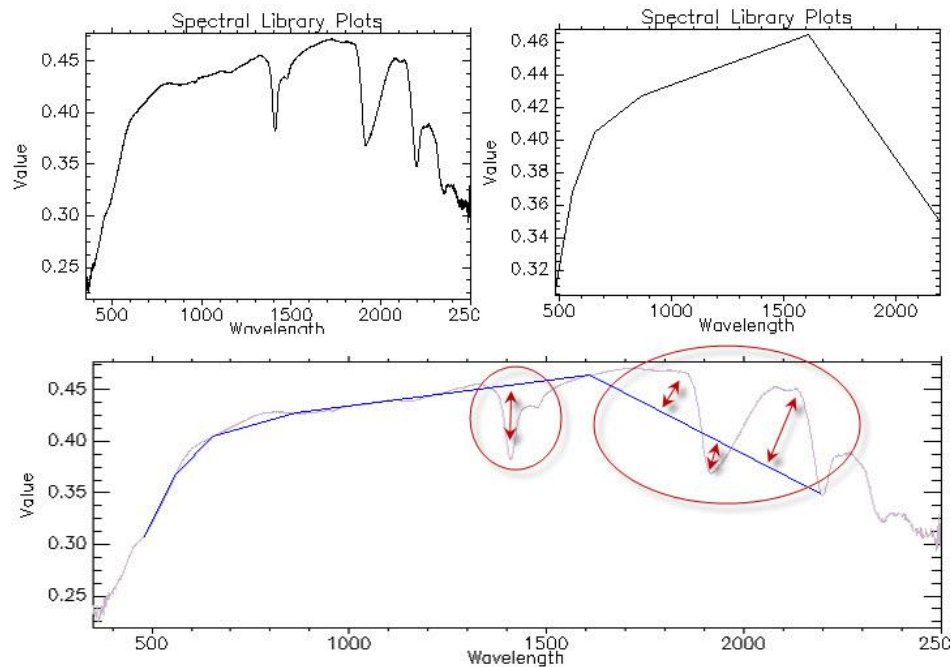


Figure 9. Comparison of Chahouk sample spectra

The areas of interest are parts of the image that are used to determine the threshold, classification, coverage, and other operations. Most of the time it is necessary to partially separate the image from the rest of the image. Classification operations require that parts of the image be separated into practice examples and introduced to the software. Using ROI¹ on an image, boundaries were specified and it was used in subsequent processing. To perform ROI-supervised classification, we must specify specific locations in the remote sensing data that represent the same regions. The sampling points of the Shirkuh granites, which contain a certain number of radioactive elements, are a good representative of granites with the same chemical composition. Samples were taken to determine granites similar to the laboratory spectroscopy and at this stage, they were classified according to the amount of radioactive elements, sampled on the ROI image and OLI image of the Shirkuh region was classified according to them. Figure 7 shows the result of this classification.

As shown in Fig. 10, an appropriate stratification of the Shirkuh granite is performed. Areas identical to each ROI are grouped together and seen as color. To determine the most abundant radioactive elements, use Table 1 to identify the three most abundant uranium and thorium samples in the categorized image. Based on the table showing the sampling points, the spectrum of each sample and the amount of uranium and thorium in it, three samples with the highest amount of uranium and thorium were selected. These three regions include West Manshad, south Tazerjan and southwest Manshad. Figure 11 is an image obtained from the Shirkuh Granite Classification using the ROI of the three zones with the most uranium and thorium. In this figure, the same group as the western sample of Manshad is characterized by the highest amount of uranium and thorium in red and the other two groups in orange and yellow, respectively.

¹ - Region of Interest

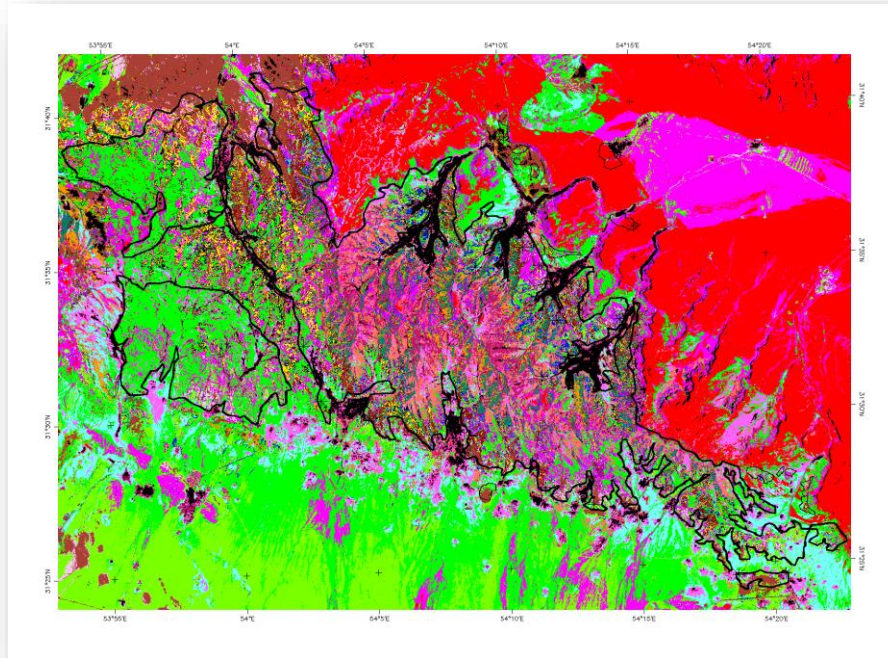


Figure 10. Supervised classification by ROI

Figure 11 is an image obtained from the Shirkuh granite classification using the ROI shows three zones with the most uranium and thorium. In this figure, the same group as the western sample due to containing the greatest amounts of uranium and thorium is indicated by red color, and the other two by orange and yellow, respectively. As shown in Fig. 11, the areas with the largest amounts of uranium and thorium are located side by side at the center of the granite mass. It can be said that due to the abundance of radioactive elements and their proximity, the chemical composition of this range of Shirkuh granite is very similar. These areas will cause the most damage to their residents. Three specimens identified in the earlier stages showed the highest hazard of radiogenic elements. Now, by identifying the locations similar to the sampling and classifying them, it is clear that the residents of Manshad, Tang Chenar, Tazrjan, Deh-Bala and Banadak Sadat Abadan are more exposed to radioactive elements than others.

As shown in Fig. 11, the areas with the largest amounts of uranium and thorium are located side by side at the center of the granite mass. It can be said that due to the abundance of radioactive elements and their proximity, the chemical composition of this range of Shirkuh granite is very similar. These areas will cause the most damage to their residents.

Three specimens identified in the earlier stages showed the highest risk of radionuclides. Now, by identifying the similarities with the sampling and classifying them, it was found that the inhabitants of Manshad, Tang-e- Chenar, Tazerjan, Dehbala and Banadak Sadat were more exposed to radioactive elements than others.

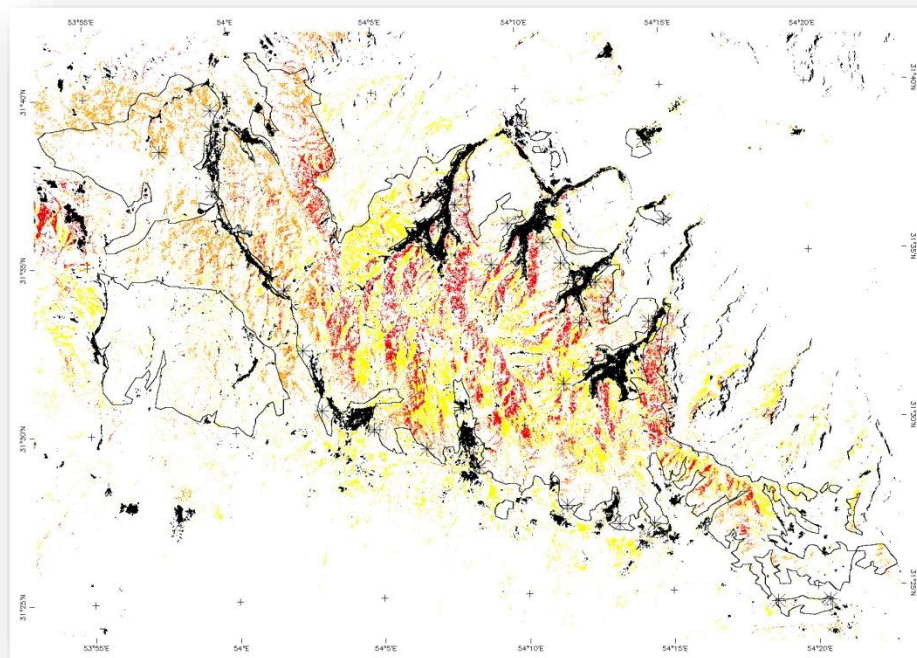


Figure 11. Three zones with the highest amount of Uranium and Thorium

4. Conclusion

One of the natural sources of radiation is granite rock, which can have radiation hazards to humans. The process of formation and accumulation of radioactive elements in the Shirkuh region of Yazd is following known geological and Petrogenesis processes. The amount of this accumulation in the granitic mass has been determined through sampling and laboratory studies. In order to avoid endangering the residents around the Shirkouh Granitic Massif that are exposed to long-term exposure to radioactive elements, they are more at risk than residents in remote areas this study determined the maximum radiation levels by examining the number of radioactive elements in the rocks of these areas. For this purpose, 30 samples with the number of radioactive elements identified by Field Spec were sampled and spectral libraries were prepared. In this study, the areas with the highest concentration of radioactive elements were identified using spectral angle mapping and supervised classification using Landsat 8 satellite images. Based on the spectral chart of the sampling points and the amount of uranium and thorium in it, the areas with the highest accumulation of radioactive elements were identified and categorized. And the results show that samples with the highest amount of uranium and thorium are more prevalent in three regions including west, south of Manshad and south of Tezerjan. In order to be more precise, it is recommended to use accurate and corrected information in patients with cancers such as lung in determining risk areas. Also, sampling the animals that live in the area will help determine how much radionuclide is affected.

References

- Zarei, Mojtaba. (2009). Investigation of natural radionuclides in Shirkuh Granites. Masters. Yazd University.
- Shibi, Maryam & Ismaili, Dariush. (2010). Petrogenesis of Shirkuh Peraluminous Granitoids (Southwest of Yazd). *Journal of Science, University of Tehran*. Volume 35. pp. 71-83.
- Ziaazerifi, Afshar; Mehri Burned Mountain, Sina; Afzal, Peyman & Jafari, Hamid Reza. (2015). Evaluation of radionuclide scattering based on airborne radiometric geophysical data in southwest Masouleh.

- Twenty-third year. No. 91. pp. 187-194.
- Atapour, Mohammad Amin. (2014). Investigating Radon's Impact on Cancer Using Remote Sensing Images. Masters. University of Science and Research.
- Murat, M. & Mojtahedzadeh, S.H. (2011). Investigation of the Impact of Granitic Basement Radiation on Groundwater in Shirkuh Yazd Watersheds. *Proceedings of the First National Conference on Applied Water Resources Research of Iran*. Pp. 25-40.
- Aboelkhair, H., Hasan, E. & Sehsah, H. (2014). Mapping of Structurally Controlled Uranium Mineralization in Kadabora Granite, Central Eastern Desert, Egypt Using Remote Sensing and Gamma Ray Spectrometry Data, Faculty of Science, Geology Department, New Damietta, Egypt, 8, pp. 54-68.
- Berberian, M. & King, G. C. P., (1981). Towards a paleogeography and tectonic evolution of Iran. *Canadian Journal of Earth Sciences*, 18(10), pp. 210-265.
- Chrysafis, I.; Mallinis, G.; Gitas, I. & Tsakiri-Strati, M. (2017). Estimating Mediterranean forest parameters using multi seasonal Landsat 8 OLI imagery and an ensemble learning method, *Remote Sensing of Environment*, 199, pp. 154-166.
- Danboyi, J.A.; Hashim, M.; Beiranvandpour, A. & Ibrahim Musa, S. (2016). Utilization of Landsat-8 Data for Lithological Mapping of Basement Rocks of Plateau State North Central Nigeria, Research Institute for Sustainability and Environment (RISE), Universiti Teknologi Malaysia, *International Conference on Geomatic and Geospatial Technology (GGT)*, Kuala Lumpur, Malaysia.
- Gol Tapeh, F., Ziaian Firouzabadi, P. & Riahi Bakhtiari, H. R. (2018). Evaluation of OLI sensor data by ALTA reflectance spectroscopy capability and the use of virtual station concept in soil heavy metal concentration scattering mapping, *Journal of Geospatial Information Technology Engineering*, Vol. 5, No. 4, Winter 96, pp. 113-145.
- Guest, B., Stockli, D.F., Grove, M., Axen, G.J., Lam, P.S. & Hassanzadeh, J. (2006). Thermal histories from the central Alborz Mountains, northern Iran: Implications for the spatial and temporal distribution of deformation in northern Iran, *Geological Society of America, Bulletin*, 118, pp. 1507-1521.
- Longhi, I., Sgavetti, M., Chiari, R. & Mazzaoli, C. (2001). Spectral Analysis and Classification of Metamorphic Rocks from Laboratory Reflectance Spectra in the 0.4-2.5 μm Interval: A Tool for Hyperspectral Data Interpretation, Taylor & Francis Ltd. *INT. J. REMOTE SENSING.*, 22, pp. 3763-3782.
- Mulloy, K.B., James, D.S., Mohs, K. & Kornfeld, M. (2001). Lung cancer in a Nonsmoking Underground Uranium Mine, *Environmental Health Perspective*, 109, pp. 305-309.
- Najafzadeh, A., Erfanian, M., Alijanpour, A. & Babaei Hesar, S. (2017). Recovering missing pixels for a Landsat SLC-off image using Weighted Linear Regression and accuracy assessment of land cover map (Case study: Khoy region, Northwest Iran), *Journal of Forest Research and Development*, 3(3), pp. 275-289.
- Qiu, Z., Hou, D., Uchida, K. & Saitoh, E. (2015). Influence of interface condition on spin-Seebeck effects, *Journal of Physics*, 48, pp. 5-21.
- Salvi, S., Mazzarini, F. & Doumaz, F. (2001). Spectral Reflectance Measurements of Geological Materials in Northern Victoria Land, Antarctica, AIT Informa, *Rivista Italiana di Telerilevamento*, 23, pp. 45-54.
- Villaseca, C., Barbero L. & Herreros V. (1998). A re-examination of the typology of per aluminous granite types in intracontinental orogenic belts, *Trans. R. Soc. Edinb. Earth Sci*, 89, pp. 113-119.